JACS
JOURNAL OF THE AMERICAN CHEMICAL SOCIETY
pubs.acs.org/JACS
Article

Carbene Complexes of Neptunium

Conrad A. P. Goodwin, Ashley J. Wooles, Jesse Murillo, Erli Lu, Josef T. Boronski, Brian L. Scott, Andrew J. Gaunt,* and Stephen T. Liddle*

Cite This: J. Am. Chem. Soc. 2022, 144, 9764–9774
Read Online
ACCESS | Metrics & More | Article Recommendations | Supporting Information

ABSTRACT: Since the advent of organotransuranium chemistry six decades ago, structurally verified complexes remain restricted to π-bonded carbocycle and σ-bonded hydrocarbyl derivatives. Thus, transuranium-carbon multiple or dative bonds are yet to be reported. Here, utilizing diphosphoniomethanide precursors we report the synthesis and characterization of transuranium-carbene derivatives, namely, diphosphonio-alkylidene- and *N*-heterocyclic carbene−neptunium(III) complexes that exhibit polarized-covalent $\sigma^2\pi^2$ multiple and dative σ^2 single transuranium-carbon bond interactions, respectively. The reaction of $[Np^{III}I_3(THF)_4]$ with $[Rb(BIPM^{TMS}H)]$ ($BIPM^{TMS}H$ = $\{HC(PPh_2NSiMe_3)_2\}^{1-}$) affords $[(BIPM^{TMS}H)Np^{III}(I)_2(THF)]$ (**3Np**) in situ, and subsequent treatment with the *N*-heterocyclic carbene $\{C(NMeCMe)_2\}$ (I^{Me4}) allows isolation of $[(BIPM^{TMS}H)Np^{III}(I)_2(I^{Me4})]$ (**4Np**). Separate treatment of in situ prepared **3Np** with benzyl potassium in 1,2-dimethoxyethane (DME) affords $[(BIPM^{TMS})Np^{III}(I)(DME)]$ (**5Np**, $BIPM^{TMS}$ = $\{C(PPh_2NSiMe_3)_2\}^{2-}$). Analogously, addition of benzyl potassium and I^{Me4} to **4Np** gives $[(BIPM^{TMS})Np^{III}(I)(I^{Me4})_2]$ (**6Np**). The synthesis of **3Np**−**6Np** was facilitated by adopting a scaled-down prechoreographed approach using cerium synthetic surrogates. The thorium(III) and uranium(III) analogues of these neptunium(III) complexes are currently unavailable, meaning that the synthesis of **4Np**−**6Np** provides an example of experimental grounding of 5f- vs 5f- and 5f- vs 4f-element bonding and reactivity comparisons being led by nonaqueous transuranium chemistry rather than thorium and uranium congeners. Computational analysis suggests that these Np^{III}=C bonds are more covalent than U^{III}=C, Ce^{III}=C, and Pm^{III}=C congeners but comparable to analogous U^{IV}=C bonds in terms of bond orders and total metal contributions to the M=C bonds. A preliminary assessment of Np^{III}=C reactivity has introduced multiple bond metathesis to transuranium chemistry, extending the range of known metallo-Wittig reactions to encompass actinide oxidation states III-VI.

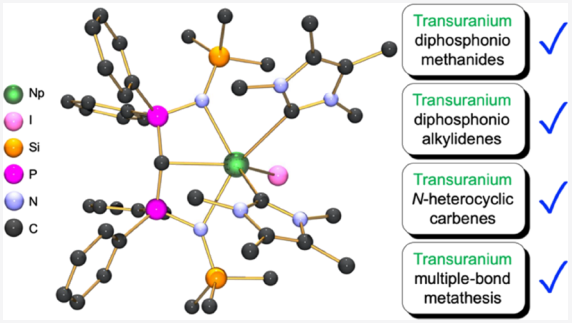

INTRODUCTION

The growing wealth of structurally authenticated Th and U covalent multiple bond chemistry that has been realized in recent years has redrawn the known boundaries and molecular-level comprehension of these early members of the 5f-block actinide (An) series.[1−4] In contrast, structurally authenticated examples of molecular non-dioxo(actinyl) transuranium-element multiple bonds are limited to a high-valent Np^{V} bis(imido) complex,[5] that is, an isolobal *N*-donor actinyl analogue, and one Np^{V} terminal mono(oxo) complex.[6] Low-valent transuranium-element multiple bonds remain restricted to spectroscopically detected $[AnE]^{n+}$ (E = O, S; n = 0−2) species.[7−13] Indeed, in contrast to the dominance of lanthanide (Ln) chemistry in the trivalent state, An-ligand (L) multiple bonding is generally found for $An^{IV\text{-}VI}$ ions. Nonetheless, with more attention given to the pursuit of transuranium-ligand multiply bonded motifs it may be possible to access An^{III}=L/An^{IV}=L and An^{III}=L/Ln^{III}=L comparisons that are currently not possible from the study of Th and U alone. The mixed-valent hexauranium ring complexes $[\{U^{III}(BIPM^{TMS})\}_3\{U^{IV}(BIPM^{TMS})\}_3(\mu\text{-I})_3(\mu\text{-}\eta^6\text{:}\eta^6\text{-}C_6H_5R)_3]$ ($(BIPM^{TMS})^{2-}$ = $\{C(PPh_2NSiMe_3)_2\}^{2-}$, a bis-(iminophosporano)methanediide; R = H, CH_3), formally containing U^{III}=C bonds represent examples of U^{III}-ligand multiple bonding, but the presence of noninnocent arene bridges clouds assignments.[14] Although organotransuranium chemistry has begun to mature over the past 5 years or so, this still sparsely populated area remains dominated by π-bonded ligands, such as the venerable cyclopentadienyl, arene, and cyclooctatetraenyl ligand sets,[15−37] and only two σ-bonded hydrocarbyl Np complexes have been structurally validated.[38,39]

As fundamental species in organometallic chemistry,[40] there is enduring interest in the chemistry of metal-carbene complexes; for example, Fischer carbenes, and of particular pertinence to this work polarized-covalent M=C double bonds, that is, alkylidenes, and dative M ← C bonds such as

Received: February 24, 2022
Published: May 24, 2022

https://doi.org/10.1021/jacs.2c02152
J. Am. Chem. Soc. 2022, 144, 9764−9774

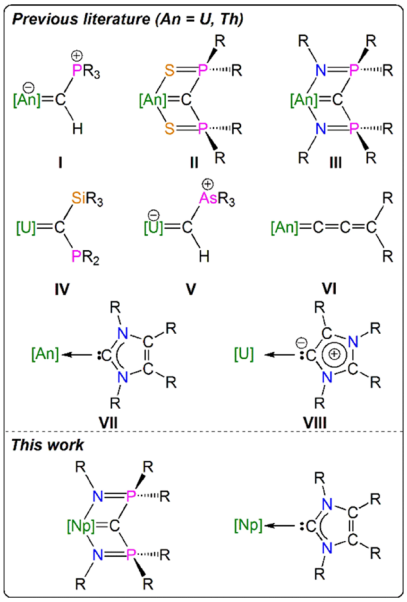

Figure 1. Key An=C and An ← C linkage types in early An-chemistry reported previously and in this work. Use of bracketed [An] (An = U or Th), [U], and [Np] is to acknowledge the various range of metal oxidation states and coligands that are omitted for clarity.

those from *N*-heterocyclic carbene (NHC) complexes.[40−45] The first structurally characterized An-carbene complex was the phosphonio-alkylidene complex $[U^{IV}(CHPMe_2Ph)(\eta^5\text{-}C_5H_5)_3]$ reported in 1981 (Figure 1, type **I**).[46] Subsequently, a range of phosphonio- and diphosphonio-alkylidene complexes of U and Th have emerged (Figure 1, type **II** and **III**),[41,47,48] and more recently, phosphino-silyl-alkylidene $(\{C(PPh_2)(SiMe_3)\}^{2-})$,[49−51] arsonium-alkylidene $(\{CHAsPh_3\}^{1-})$,[52] and allenylidene $(\{CCCPh_2\}^{2-})$[53] derivatives have been reported (Figure 1, type **IV-VI**). The first An-NHC complexes (Figure 1, type **VII**), $[UO_2Cl_2\{C(NMesCX)_2\}_2]$ (Mes = 2,4,6-$Me_3C_6H_2$; X = H or Cl), were reported in 2001.[54,55] More recently, the $\{C(NMeCMe)_2\}$ (I^{Me4}) NHC has proven to be useful for supporting uranium(III)[56] and (IV)[57,58] and for providing comparison to mesoionic carbene derivatives (Figure 1, type **VIII**).[59] To date, there are no transuranium-carbon multiple bonds for any transuranium oxidation state and no transuranium-NHC complexes.

Here, we report the preparation of a diphosphoniomethanide-Np complex, which contains a polarized-covalent transuranium-carbon single σ^2-bond. This methanide complex provides an entry-point to transuranium-carbene complexes, including two diphosphonio-alkylidene-Np^{III} and two Np^{III}-NHC derivatives that constitute transuranium-carbon polarized-covalent $\sigma^2\pi^2$ multiple bond and dative σ^2 single bond interactions, respectively, Figure 1. The synthesis of these low-valent Np complexes produces clear-cut An^{III}-ligand multiple bonding free of redox-active ancillary ligands and was facilitated by adopting a scaled-down prechoreographed approach using Ce as a synthetic surrogate. The analogous Th and U complexes remain experimentally unavailable, and so these Np complexes provide an instance where, instead of Th and U, it is low-valent transuranium chemistry that provides the precedent for experimentally benchmarking comparisons of homologous 5f and 4f electronic structure and bonding.

RESULTS AND DISCUSSION

Synthetic Considerations. Previously, we found that the reaction of half an equivalent of $[Li_2\{C(PPh_2NSiMe_3)_2\}]_2$ ($[Li_2BIPM^{TMS}]_2$) with $[U^{IV}Cl_4(THF)_3]$ straightforwardly and reliably afforded $[(BIPM^{TMS})U^{IV}(Cl)(\mu\text{-}Cl)_2Li(THF)_2]$ or $[\{(BIPM^{TMS})U^{IV}(Cl)(\mu\text{-}Cl)(THF)\}_2]$ depending on the work-up conditions employed.[60−62] In contrast, we find that the analogous reaction between $[Li_2BIPM^{TMS}]_2$ and $[Np^{IV}Cl_4(DME)_2]$, Scheme 1a, mostly results in intractable, dark product mixtures. However, a small crop of crystals of $[(BIPM^{TMS}H)Np^{III}(Cl)(\mu\text{-}Cl)_3Np^{III}\{\mu\text{-}(Cl)Li(DME)(OEt_2)\}(BIPM^{TMS}H)]$ (**1**) was isolated on one occasion. Here, Np^{IV} has been reduced to Np^{III}, and each $(BIPM^{TMS})^{2-}$ dianion has become protonated to its $(BIPM^{TMS}H)^{1-}$ anion form $((BIPM^{TMS}H)^{1-} = \{HC(PPh_2NSiMe_3)_2\}^{1-}$, a bis-(iminophosphorano)methanide). We note that repeating the reaction under identical conditions, except using $[U^{IV}Cl_4(DME)_2]$ instead of $[Np^{IV}Cl_4(DME)_2]$, results in the isolation of $[\{(BIPM^{TMS})U^{IV}\}_2(\mu\text{-}Cl)_6\{Li(DME)\}_2]$ (**2**), analogously to our earlier reports.[60−62] In this case, U^{IV} ions are

Scheme 1. Synthesis of 1, 2, and 3M−6M (M = Ce, Np)[a]

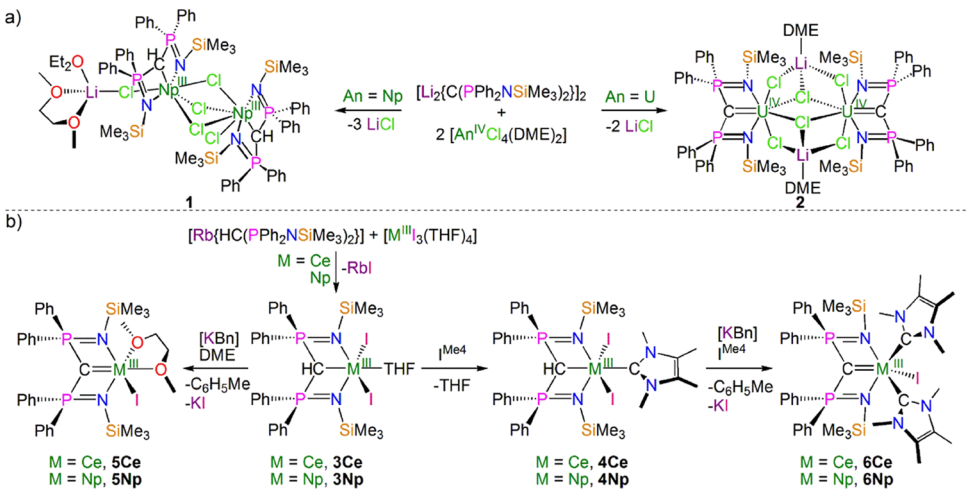

[a]Complex **3Np** was not isolated. DME = 1,2-dimethoxyethane; Bn = benzyl; $I^{Me4} = \{C(NMeCMe)_2\}$.

https://doi.org/10.1021/jacs.2c02152
J. Am. Chem. Soc. 2022, 144, 9764−9774

retained and no protonation of the $(BIPM^{TMS})^{2-}$ dianion occurs, Scheme 1a. These different observations for U and Np highlight the greater redox stability of U^{IV} compared to Np^{IV},[63] but the presence of occluded LiCl in $[(BIPM^{TMS})U^{IV}(Cl)(\mu\text{-}Cl)_2Li(THF)_2]$ and **2** also suggested that using Li/Cl combinations could complicate reaction product outcomes. We therefore concluded that Li-reagents should be avoided and that a Np^{III} starting material could facilitate a rational route to access Np=C bonds without undesired redox chemistry.

We identified $[Np^{III}I_3(THF)_4]$ as a suitable starting material from which Np=C bonds could be prepared using $BIPM^{TMS}$, given that a new, convenient Np^0-metal-free route was recently reported to access this starting material.[64] The combination of limited Np stocks (in comparison to Th, U, and Ln materials) coupled with the relatively high-specific radioactivity of ^{237}Np, and its daughter isotopes, necessitated a small-scale use strategy (typically <30 mg Np) and preoptimized reaction and crystallization conditions based on surrogate trials. Thus, to manage the use of valuable Np we first choreographed scaled-down reactions using $[Ce^{III}I_3(THF)_4]$ as a synthetic surrogate for $[Np^{III}I_3(THF)_4]$. The synthesis of $[(BIPM^{TMS}H)Ce^{III}(I)_2(THF)]$ (**3Ce**) using $[Rb(BIPM^{TMS}H)]$ and $[Ce^{III}I_3(THF)_4]$ on multigram (>10 mmol) scales has been reported previously.[65] To determine compatibility with our Np experimental protocols, we optimized the synthesis of **3Ce** with those reagents at ∼0.04 mmol scale, Scheme 1b, and found that on this scale reactions can be performed rapidly and still yield crystalline **3Ce**. During reaction optimizations, we noted that the THF in **3Ce** is seemingly labile presenting opportunities for decomposition, which can present a major impediment on small scales. We therefore prepared the new derivative $[(BIPM^{TMS}H)Ce^{III}(I)_2(I^{Me4})]$ (**4Ce**, I^{Me4} = {C(NMeCMe)$_2$}), Scheme 1b, because the I^{Me4} is a strong, kinetically inert donor and its use would pave the way to introducing NHC ligands to transuranium chemistry. With small-scale preparations of crystalline **3Ce** and **4Ce** in hand, we treated each with benzyl potassium in the presence of DME and I^{Me4},[66,67] respectively, yielding crystalline samples of previously reported $[(BIPM^{TMS})Ce^{III}(I)(DME)]$ (**5Ce**) and the new derivative $[(BIPM^{TMS})Ce^{III}(I)(I^{Me4})_2]$ (**6Ce**), Scheme 1b.

With the small-scale synthesis of **3Ce**−**6Ce** accomplished, we attempted the synthesis of the Np^{III} analogues, Scheme 1b. At a small scale (∼0.03−0.04 mmol of Np), utilizing $[Rb(BIPM^{TMS}H)]$ and $[Np^{III}I_3(THF)_4]$ we could not isolate $[(BIPM^{TMS}H)Np^{III}(I)_2(THF)]$ (**3 Np**), possibly because of the THF-lability issue observed for **3Ce**. However, adding I^{Me4} to **3Np** prepared in situ afforded $[(BIPM^{TMS}H)Np^{III}(I)_2(I^{Me4})]$ (**4 Np**) as ruby-red crystals in 16% yield. Likewise, the reaction between benzyl potassium and **3Np** (prepared in situ) in DME afforded $[(BIPM^{TMS})Np^{III}(I)(DME)]$ (**5Np**) as orange crystals in 37% isolated yield. Finally, treatment of **4Np** with benzyl potassium and I^{Me4} afforded $[(BIPM^{TMS})Np^{III}(I)(I^{Me4})_2]$ (**6Np**) as red-purple crystals in 32% yield. Though the yields are low, which is attributed to the small scales and quite soluble nature of these complexes, they are reproducible.

Previously, it has been found that U^{III} disproportionates when paired with the $(BIPM^{TMS})^{2-}$ dianion, requiring arene buffers in inverse-sandwich-arene complexes to stabilize this combination via extensive U-arene δ-bonding interactions.[14,61] We therefore revisited the synthesis of the U-analogues under these new preparative conditions using $[U^{III}I_3(THF)_4]$, because these small-scale reactions are performed quickly. Although $[(BIPM^{TMS}H)U^{III}(I)_2(THF)]$ (**3U**) can be made and isolated as per our previous report,[14] all attempts to deprotonate and isolate the resulting product either result in disproportionation and/or decomposition or the formation of inverse-sandwich-arene complexes, highlighting the intrinsically less stable nature of U^{III} compared to Np^{III}.[68] Nevertheless, the isolation of **4Np**−**6Np** permits opportunities to make experimentally benchmarked An^{III} vs An^{IV} and An^{III} vs Ln^{III} M=C (M = An, Ln) bonding comparisons that would otherwise remain lacking.[69−72]

Solid-State Structures. To define the metrical details of **4Np**−**6Np**, their solid-state molecular structures were determined by single-crystal X-ray diffraction. For completeness, and as part of the choreographing scaled-down verification process, the structures of isomorphous (for each metal pair) **3Ce**−**6Ce** were determined (see the Supporting Information for full details), noting that **3Ce** and **5Ce** were structural redeterminations, whereas those of **4Ce** and **6Ce** are reported for the first time. Before we discuss the Np−C interactions in detail, we note that the Np−N distances in **4Np**−**6Np** are either statistically indistinguishable (by the 3σ-criterion) or are only marginally shorter than the corresponding Ce−N distances in **4Ce**−**6Ce**, meaning that clear-cut conclusions cannot be drawn about any M−N bond length trends in these complexes. Where the M−I distances are concerned, the Np−I and Ce−I distances vary consistently as expected for the different coordination environments of **4Np**−**6Np** and **4Ce**−**6Ce**, but we note that for each isomorphous pair the Np−I distances are consistently shorter (∼0.02−0.05 Å) than the corresponding Ce−I distances.

The structure of **4Np**, Figure 2, reveals a highly irregular six-coordinate Np ion, where the diphosphoniomethanide ligand adopts an "open-book" geometry.[48] The two iodide ligands are approximately *trans*, though with quite an acute I-Np-I angle of 135.87(2)°, and the I^{Me4} NHC sits approximately *trans* to the methanide center, although again distorted far from the ideal (HC−Np−C_{NHC} = 134.6(2)°). The Np−CH_{BIPM} and the Np ← C_{NHC} distances are 2.753(7) and 2.678(8) Å, respectively; we note that the former is ∼0.07 Å longer than the latter, despite their respective formal anionic and neutral charge states, likely reflecting the strongly donating nature of I^{Me4} and constraints of the $(BIPM^{TMS}H)^{1-}$ anion chelate framework. The Np−CH_{BIPM} distance in **4Np** sits between the Np−C bond lengths of 2.574(4)−2.592(4) Å in $[Np^{III}\{C_6H_5C(H)NMe_2\}_3]$[39] and 2.831(4) and 2.838(4) Å in **1**, is slightly shorter than the Ce−CH_{BIPM} distance of 2.806(9) Å in **3Ce**, but is statistically indistinguishable (by the 3σ-criterion) from the Ce−CH_{BIPM} distance of 2.768(6) Å in isostructural **4Ce**; as expected, all are longer than the Np−C bonds (2.440(10) and 2.454(12) Å) in a previously reported Np^{IV} silylamide double cyclometallate complex.[38] The Np−CH_{BIPM} distance in **4Np** is ∼0.08 Å shorter than the U−CH_{BIPM} distance of 2.827(3) Å in **3 U**. However, we note that the M−CH_{BIPM} distance in **3U** is ∼0.02 Å longer than the corresponding distance in **3Ce**, as expected from Shannon's revised ionic radii (6-coordinate ions, Ce = 1.01; U = 1.03 Å)[73] so it seems likely that the different M−CH_{BIPM} distances in **4Np** and **3U** reflect the absence of the NHC ligand in the latter rather than an underlying Np vs U difference. There are no transuranium-NHC distances with which to compare the Np−C_{NHC} distance in **4Np**, but we note that the U ← C_{NHC} distance in $[U\{N(SiMe_3)_2\}_3(I^{Me4})]$[56] is

https://doi.org/10.1021/jacs.2c02152
J. Am. Chem. Soc. 2022, 144, 9764−9774

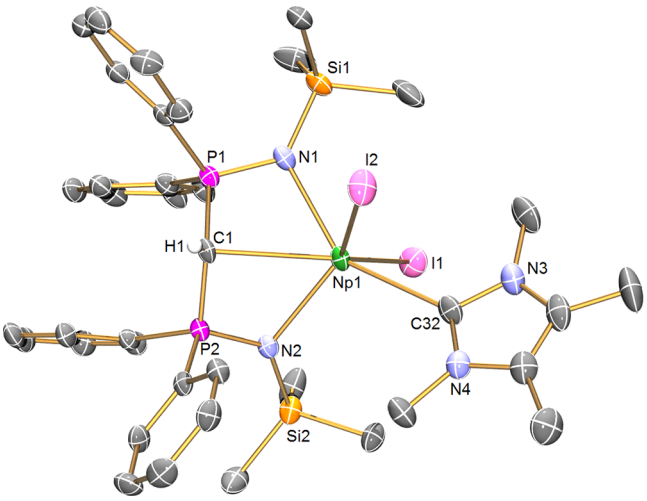

Figure 2. Solid-state molecular structure of complex **4Np** at 100 K. Displacement ellipsoids are set at 50% probability and nonmethanide hydrogen atoms are omitted for clarity. Selected bond lengths [Å] and angles [°]: Np1-I1 3.0727(6), Np1-I2 3.1798(6), Np1-N1 2.423(6), Np1-N2 2.458(6), Np1-C1 2.753(7), Np1-C32 2.676(8), P1-N1 1.612(6), P1-C1 1.749(7), P2-N2 1.618(6), P2-C1 1.723(7), I1-Np1-I2 135.87(2), N1-Np1-I1 93.1(2), N1-Np1-I2 84.7(12), N1-Np1-N2 105.8(2), N1-Np1-C1 63.3(2), N1-Np1-C32 144.1(2), N2-Np1-I1 91.1(2), N2-Np1-I2 131.9(2), N2-Np1-C1 62.0(2), N2-Np1-C32 110.0(2), C1-Np1-I1 133.8(2), C1-Np1-I2 83.8(2), C32-Np1-I1 88.2(2), C32-Np1-I2 70.0(2), C32-Np1-C1 134.6(2), and P1-C1-P2 128.6(4).

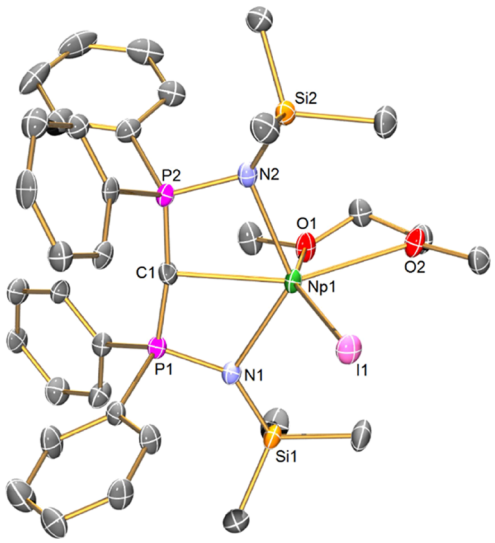

Figure 3. Solid-state molecular structure of complex **5Np** at 100 K. Displacement ellipsoids are set at 50% probability and hydrogen atoms and lattice solvent are omitted for clarity. Selected bond lengths [Å] and angles [°]: Np1-I1 3.1065(5), Np1-O1 2.524(5), Np1-O2 2.636(5), Np1-N1 2.431(6), Np1-N2 2.414(6), Np1-C1 2.425(7), P1-N1 1.602(6), P1-C1 1.627(7), P2-N2 1.631(6), P2-C1 1.652(7), O1-Np1-I1 153.9(2), O1-Np1-O2 61.8(2), O2-Np1-I1 95.3(2), N1-Np1-I1 103.6(2), N1-Np1-O1 81.3(2), N1-Np1-O2 122.4(2), N2-Np1-I1 95.2(2), N2-Np1-O1 101.5(2), N2-Np1-O2 102.2(2), N2-Np1-N1 128.8(2), N2-Np1-C1 65.2(2), C1-Np1-I1 109.3(2), C1-Np1-O1 95.9(2), C1-Np1-O2 152.9(2), C1-Np1-N1 63.6(2), and P1-C1-P2 170.4(5).

statistically indistinguishable at 2.672(5) Å. The Ce ← C_{NHC} distance of 2.731(8) Å in **4Ce** is significantly (~0.06 Å) longer than the analogous distance in **4Np** even though according to Shannon's revised ionic radii, six-coordinate Ce and Np are both 1.01 Å.[62]

The structure of **5Np**, Figure 3, reveals a distorted octahedral Np ion, where the diphosphonio-alkylidene C-center is *trans* to a DME oxygen donor atom, the iodide is *trans* to the other DME oxygen donor atom, and the nitrogen donors can be considered to be *trans* to one another. Notably, the iodide is thus oriented *cis* with respect to the diphosphonio-alkylidene C-atom. The carbene adopts a T-shaped geometry, with a P-C-P angle of 170.4(5)° and a sum of angles at the C_{BIPM} center of 359.9°, which in principle orients it favorably to engage in a double-bonding interaction with Np. The Np−C_{BIPM} distance is found to be 2.425(7) Å. There is no transuranium precedent to compare the Np═C_{BIPM} distance in **5Np** to; however, we note that the Ce═C_{BIPM} distance in isostructural **5Ce** (2.477(2) Å) is longer by 0.052(2) Å. The Np═C_{BIPM} distance in **5Np** fits nicely into the trend established by previous U═C_{BIPM} complexes, with, for example, $[U^{VI}(BIPM^{TMS})(Cl)_2(O)]$, U^{VI}═C = 2.184(3) Å; $[U^{V}(BIPM^{TMS})(Cl)_2(I)]$, U^{V}═C = 2.268(10) Å; $[\{U^{IV}(BIPM^{TMS})(\mu\text{-}Cl)(Cl)(THF)\}_2]$, U^{IV}═C = 2.322(4) Å; $[\{U^{III}(BIPM^{TMS})\}_3\{U^{IV}(BIPM^{TMS})\}_3(\mu\text{-}I)_3(\mu\text{-}\eta^6{:}\eta^6\text{-}C_7H_8)_3]$, U^{III}═C = 2.413(8) and 2.47(2) Å, U^{IV}═C = 2.398(7) and 2.30(3) Å.[60,61] The P−C distances in **5Np** (av. 1.640 Å) are contracted (~0.1 Å) compared to the P−C distances in **4Np** (av. 1.736 Å), reflecting the increased charge at the central carbon atom of $(BIPM^{TMS})^{2-}$ in **5Np** instead of $(BIPM^{TMS}H)^{1-}$ in **4Np**. This can be rationalized by invoking dipolar electrostatic shortening rather than hyperconjugation or delocalization effects.[74]

The structure of **6Np**, Figure 4, reveals an irregular six-coordinate Np ion, where the diphosphonio-alkylidene adopts an open book geometry,[48] the two I^{Me4} NHCs are *cis* with respect to each other residing on the more open face presented by the $(BIPM^{TMS})^{2-}$ ligand, and the iodide resides on the opposite, more closed face. The P-C-P angle is 136.5(3)° and the sum of angles at the C_{BIPM} center is 322.5°. This pyramidalization of the C_{BIPM} in principle would be expected to make it a poorer donor center than the one in **5Np**, which is consistent with the Np═C_{BIPM} distance of 2.490(6) Å in **6Np**, which is ~0.07 Å longer than the corresponding Np═C_{BIPM} distance in **5Np**; the pyramidalization of the C_{BIPM} center may reflect steric congestion and also that with so many strong donors the Np ion in **6Np** may be quite electron-rich, which is consistent with the optical data (*vide infra*). Consistent with these observations, the P−C distances in **6Np** (av. 1.673 Å) are slightly (0.03 Å) longer than the P−C distances in **5Np**. Nevertheless, the Np═C_{BIPM} distance in **6Np** is slightly shorter than the corresponding Ce═C_{BIPM} distance of 2.519(2) Å in isostructural **6Ce**. The two Np ← C_{NHC} distances are 2.677(5) and 2.751(6) Å − clearly longer than the formal Np═C_{BIPM} distance, and one is statistically indistinguishable to the analogous Np ← C_{NHC} distance in **4Np**. One Np ← C_{NHC} distance is indistinguishable from the U ← C_{NHC} distance in $[U\{N(SiMe_3)_2\}_3(I^{Me4})]$, but the other is ~0.07 Å longer, likely reflecting steric congestion at the Np ion. This pattern is also found in isostructural **6Ce** with Ce ← C_{NHC} distances of 2.737(3) and 2.806(2) Å, revealing that the Np ← C_{NHC} distances in **6Np** are consistently ~0.06 Å shorter than the Ce ← C_{NHC} distances in **6Ce** despite the identical Shannon ionic radii of Np and Ce.

https://doi.org/10.1021/jacs.2c02152
J. Am. Chem. Soc. 2022, 144, 9764−9774

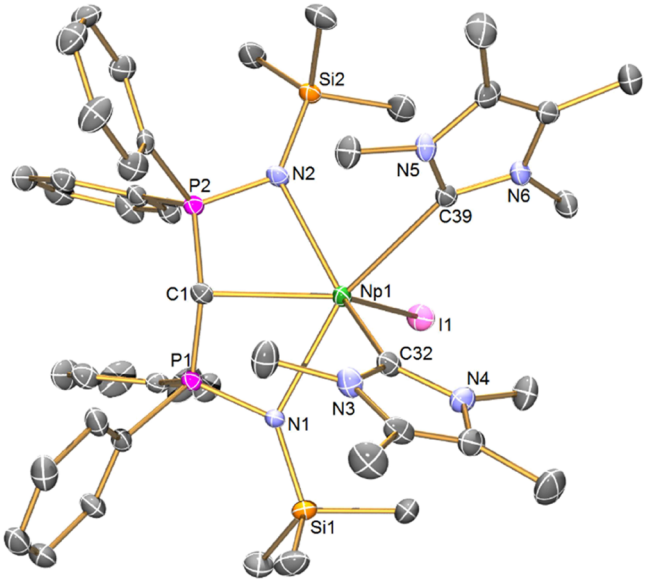

Figure 4. Solid-state molecular structure of complex **6Np** at 120 K. Displacement ellipsoids are set at 50% probability and hydrogen atoms and lattice solvent are omitted for clarity. Selected bond lengths [Å] and angles [°]: Np1-I1 3.1571(4), Np1-N1 2.485(4), Np1-N2 2.492(5), Np1-C1 2.490(6), Np1-C32 2.677(5), Np1-C39 2.751(6), P1-N1 1.620(5), P1-C1 1.675(6), P2-N2 1.614(5), P2-C1 1.671(5), N1-Np1-I1 91.8(2), N1-Np1-N2 120.9(2), N1-Np1-C1 64.0(2), N1-Np1-C32 81.4(2), N1-Np1-C39 154.2(2), N2-Np1-I1 98.1(2), N2-Np1-C32 132.7(2), N2-Np1-C39 81.0(2), C1-Np1-I1 127.5(2), C1-Np1-N2 64.1(2), C1-Np1-C32 98.7(2), C1-Np1-C39 123.6(2), C32-Np1-I1 124.3(2), C32-Np1-C39 73.2(2), C39-Np1-I1 98.7(2), and P1-C1-P2 136.5(3).

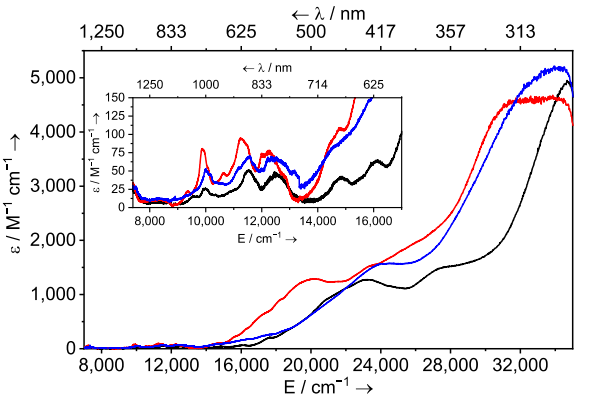

Figure 5. Comparison of solution UV−vis−NIR spectra of **4Np** (black line, 0.49 mM), **5Np** (blue line, 0.51 mM), and **6Np** (red line, 0.58 mM), all in toluene shown between 7000 and 35,000 cm^{-1} (1429−286 nm) at ambient temperature. Inset: Expanded view of ~8000−16,000 cm^{-1} region.

Overall, the solid-state molecular structures for **4Np−6Np** reveal that there are no substantial differences between Np^{III} and U^{III} where these Np−CH_{BIPM}, Np=C_{BIPM}, and Np ← C_{NHC} distances are concerned − at least across the small range of comparable molecules. However, a clear trend emerges where Np exhibits consistently shorter Np=C_{BIPM} and Np ← C_{NHC} distances (~0.03 and ~0.06 Å, respectively) compared to isostructural Ce=C_{BIPM} and Ce ← C_{NHC} distances. The Np−CH_{BIPM} and Ce−CH_{BIPM} distances do not exhibit any statistically significant differences. While $(BIPM^{TMS})^{2-}$ enjoys considerable conformational flexibility, allowing facile variation in its donor strength to metals, and hence M=C distances, $(BIPM^{TMS}H)^{1-}$ is more rigid. Thus, the similarity in Np−CH_{BIPM} and Ce−CH_{BIPM} bond distances likely reflects the constraints of this chelate.

Spectroscopic Analysis. The ^1H nuclear magnetic resonance (NMR) spectra of **4Np−6Np** are consistent with their Np^{III} $5f^4$ formulations, exhibiting paramagnetically shifted resonances in spectral windows up to 67 ppm. In particular, the CH_{BIPM} resonance for **4Np** is found at −54.6 ppm. The ^{31}P NMR spectra are also characteristically paramagnetically shifted, and it is notable that the ^{31}P chemical shift for **4Np** (−488 ppm) shifts significantly when converted to **5Np** and **6Np** (−789 and −740 ppm), which for the latter are similar chemical shifts to $[BIPM^{TMS}U^{IV}(X)_n]$ complexes (X = alkyl, amide, imido; n = 2, 2, 1, respectively) which are $5f^2$ congeners that typically span the range −605 to −905 ppm.[75−77]

The UV−vis−NIR spectra of **4Np−6Np**, Figure 5, are consistent with those of their Np^{III} formulations.[6,38,64,71,78−80] In particular, broad pairs of absorptions, presumed to be Laporte allowed f-d transitions, are found in the 16,000−26,000 cm^{-1} region (ε = ~1500 M^{-1} cm^{-1}). As the ligand fields change from **4Np** to **5Np** to **6Np** the pairs of bands shift and can be ordered energetically as **5Np** > **4Np** > **6Np**. The most electron-rich Np would, simplistically, be expected to have the smallest f-d energy gap, and indeed, this is consistent with the ligand field at **6Np** and that the pair of f-d absorptions for **6Np** are lowest in energy of the series. While comparisons using **5Np** are complicated by it being the sole complex with DME in the coordination sphere of Np, **4Np** and **6Np** are more closely related, with BIPM, iodide, and NHC ligands common to both and here the f-d energy ordering of **5Np** > **6Np** is clear, reflecting the presence of the strongly donating diphosphonio-alkylidene in the latter. The NIR regions of the UV−vis−NIR spectra of **4Np−6Np**, Figure 5 inset, exhibit multiple weak absorptions assigned as Laporte forbidden f-f transitions whose overall patterns are characteristic of Np^{III}.[6,38,64,71,78−80] The absorption bands at ~10,000, ~11,500, and ~12,500 cm^{-1} can be assigned to the $^5I_7$, $^5F_3$, and $^5G_3/^5I_8/^5S_2$ transitions of Np^{III},[81] and we note that the intensities and fwhm values for **5Np** (ε = ~90 M^{-1} cm^{-1}, fwhm = 530, 1000, 1108, av. 879 cm^{-1}) and **6Np** (ε = ~75 M^{-1} cm^{-1}, fwhm = 426, 909, 1095, av. 810 cm^{-1}) are slightly larger than those for **4Np** (ε = ~50 M^{-1} cm^{-1}, fwhm = 418, 842, 1045, av. 768 cm^{-1}). Though the changes are modest, this may reflect the presence of the strong diphosphonio-alkylidene donors in the former pair compared to the diphosphoniomethanide in the latter, which in turn would invoke Np 5f-orbital contributions to the bonding of these complexes, which is indeed supported by density functional theory (DFT) calculations (*vide infra*).

Quantum Chemical Calculations. To probe the nature of the Np−C interactions in **4Np−6Np**, we performed DFT calculations. Because **4Np−6Np** are experimentally authenticated, we calculated the experimentally inaccessible, and hence hypothetical, **4U−6U** complexes, using structurally validated **4Np−6Np** to give confidence in the DFT results and provide $5f^3$ U^{III} vs $5f^4$ Np^{III} comparisons. Given the ionic radii size match of Np^{III} and Ce^{III}, and with **4Ce−6Ce** structurally authenticated, we also performed DFT calculations on **4Ce−6Ce** to provide an isostructural Ln^{III} vs An^{III} comparison. Noting that Ce^{III} is a good size match to Np^{III}, but with different f-electron counts of $4f^1$ and $5f^4$, respectively, we also

https://doi.org/10.1021/jacs.2c02152
J. Am. Chem. Soc. 2022, 144, 9764−9774

Table 1. Selected Computed Properties for 4M−6M (M = Np, U, Ce, Pm)

	bond and indices		charges[d]		spin densities[e]		NBO M-C σ-bond component (%)[f]			NBO M-C π-bond component (%)[f]			QTAIM[h]	
Cmpd[a]	bond[b]	BI[c]	M	C	M	C	M[g]	C[g]	M s/p/d/f	M	C	M s/p/d/f	ρ	ε
4Np	Np−CH_{BIPM}	0.59	1.51	−1.64	4.21	−0.01	9	91	9/0/45/46				0.04	0.05
	Np ← C_{NHC}	0.83		−0.43		−0.02	0	100					0.05	0.01
5Np	Np═C_{BIPM}	1.40	1.54	−1.96	4.36	−0.07	17	83	4/1/32/63	14	86	0/0/38/62	0.08	0.21
6Np	Np═C_{BIPM}	1.20	1.51	−1.64	4.22	−0.05	15	85	9/1/39/51	10	90	0/1/43/56	0.08	0.18
	Np ← C_{NHC}	0.65		−0.44		−0.03	0	100					0.04	0.03
	Np ← C_{NHC}	0.69		−0.46		−0.03	0	100					0.05	0.03
4U	U−CH_{BIPM}	0.58	1.58	−1.65	3.09	−0.01	9	91	8/0/47/45				0.04	0.05
	U ← C_{NHC}	0.82		−0.45		−0.02	0	100					0.05	0.01
5U	U═C_{BIPM}	1.28	1.57	−2.00	3.28	−0.04	14	86	4/1/42/53	13	87	0/0/40/60	0.08	0.20
6U	U═C_{BIPM}	1.17	1.62	−1.67	3.08	−0.04	14	86	10/1/46/43	10	90	0/1/50/49	0.08	0.17
	U ← C_{NHC}	0.77		−0.50		−0.03	0	100					0.05	0.03
	U ← C_{NHC}	0.81		−0.48		−0.03	0	100					0.05	0.03
4Ce	Ce−CH_{BIPM}	0.46	1.20	−1.54	1.04	−0.01	0	100					0.04	0.05
	Ce ← C_{NHC}	0.60		−0.31		−0.01	0	100					0.04	0.01
5Ce	Ce═C_{BIPM}	1.05	1.32	−1.82	1.07	−0.01	10	90	1/1/61/37	8	92	0/0/65/35	0.07	0.22
6Ce	Ce═C_{BIPM}	0.96	1.29	−1.53	1.01	−0.01	9	91	7/1/65/27	7	93	2/1/60/37	0.07	0.19
	Ce ← C_{NHC}	0.52		−0.38		−0.01	0	100					0.04	0.03
	Ce ← C_{NHC}	0.58		−0.36		−0.01	0	100					0.04	0.03
4Pm	Pm−CH_{BIPM}	0.31	1.06	−1.47	4.38	−0.04	10	90	5/0/32/63				0.04	0.05
	Pm ← C_{NHC}	0.39		−0.26		−0.05	0	100					0.04	0.05
5Pm	Pm═C_{BIPM}	0.94	1.26	−1.76	4.40	−0.02	18	82	1/0/24/75	19	81	0/0/20/80	0.07	0.16
6Pm	Pm═C_{BIPM}	0.76	1.11	−1.48	4.39	−0.02	15	85	5/1/31/63	14	86	1/0/24/75	0.06	0.13
	Pm ← C_{NHC}	0.28		−0.31		−0.02	0	100					0.03	0.05
	Pm ← C_{NHC}	0.33		−0.29		−0.02	0	100					0.04	0.02

[a]All compounds geometry optimized without symmetry constraints at the BP86 TZP/ZORA (all-electron) level. [b]M−C bond: M−CH_{BIPM} = methanide of $(BIPM^{TMS}H)^{1-}$; M ← C_{NHC} = I^{Me4} NHC carbene; M═C_{BIPM} = diphosphonio-alkylidene of $(BIPM^{TMS})^{2-}$. [c]Nalewajski−Mrozek bond indices. [d]MDC_q charges. [e]MDC_m spin densities. [f]Natural bond orbital (NBO) analysis. [g]Values of 0% for the total M contribution to the M−C bond mean that the M contribution is below the cut-off threshold of NBO (5%). [h]Quantum Theory of Atoms in Molecules (QTAIM) bond critical point topological electron density (ρ) and ellipticity (ε) analysis.

performed DFT calculations on hypothetical **4Pm−6Pm** because Pm^{III} is $4f^4$ and isoelectronic to $5f^4$ Np^{III}. Confidence in the hypothetical Pm models is afforded by the structurally confirmed **4Ce−6Ce**. Given the good agreement between the gas-phase geometry optimized and solid-state metrical data, where comparisons are available, the DFT data can be considered to represent a reliable qualitative model of the electronic structures (Table 1) and hence a representative picture to probe bonding differences suggested by the solid-state metrical data. Note that there is little structural variance in the computed M−N bonding ($\Delta_{max/av.}$ +0.04/+0.02 Å between Np and Ce structures), in line with the experimental solid-state metrical data, hence we focus discussion on the M−C bond interactions.

As expected, the Np−CH_{BIPM} bond order in **4Np** (0.59) reveals a polarized linkage, but conversion of that linkage to Np═C_{BIPM} gives bond indices for **5Np** and **6Np** (1.40 and 1.20) that are at least double that of **4Np**, reflecting their formal polarized-covalent single- and double-bond natures, respectively. The dative Np ← C_{NHC} bond orders are broadly similar to the covalent Np−CH_{BIPM} bond index, reflecting the strong donor nature of I^{Me4}, but this metric is noticeably larger for the Np ← C_{NHC} bond in **4Np** (0.83) than **6Np** (av. 0.67) reflecting the weaker donor strength of $(BIPM^{TMS}H)^{1-}$ compared to $(BIPM^{TMS})^{2-}$. The computed charges and spin densities are overall consistent with Np^{III} ions (av. 1.52, 4.26, respectively) and charge donation from the ligands to Np centers. Highly electrostatic Np−CH_{BIPM} and Np ← C_{NHC} interactions are returned by NBO analyses, but polarized-covalent Np═C_{BIPM} twofold bonding interactions with Np contributions of 10−17% are confirmed, as exemplified by the Np═C_{BIPM} bond of **5Np**, Figure 6 and Table 1 (and see the Supporting Information). QTAIM analysis of **4Np−6Np**

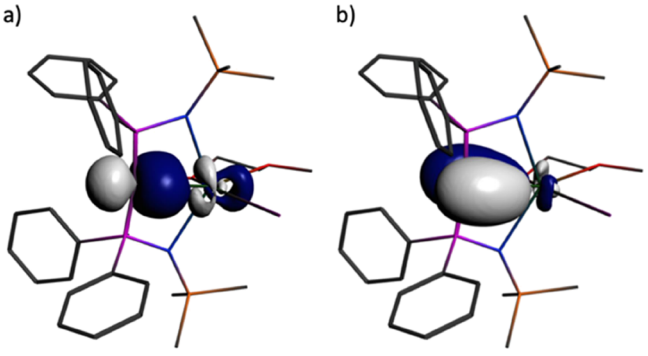

Figure 6. NBO representations of the Np═C_{BIPM} σ- and π-bond interaction in **5Np**. (a) Np═C_{BIPM} σ-bond. (b) Np═C_{BIPM} π-bond. Hydrogen atoms are omitted for clarity.

https://doi.org/10.1021/jacs.2c02152
J. Am. Chem. Soc. 2022, 144, 9764−9774

confirms the anticipated polarized-covalent nature of the Np=C_{BIPM} bonds in **5Np** and **6Np**, again with more covalent Np=C_{BIPM} than Np ← C_{NHC} bonds. The bond critical point ellipticity values reveal cylindrical single bonds for the Np−CH_{BIPM} and Np ← C_{NHC} interactions (ε values close to zero) and asymmetric double-bond interactions for the Np=C_{BIPM} linkages (ε values that deviate substantially from zero, for example, benzene and ethene have ε values of 0.23 and 0.45, respectively).[82]

Previous work on U^{IV}=C_{BIPM} complexes, using the same level of theory for the calculations on **5Np** and **6Np** (BP86, all-electron ZORA TZP), found total U^{IV} contributions averaging ∼15−18%, with bond orders of ∼1.4. Those data are remarkably similar to those found for Np^{III} **5Np** and **6Np**. To account for this, two competing effects merit consideration. For equivalent oxidation states, Np has a greater effective nuclear charge than U, so the radial distribution of the 5f- and 6d-orbitals will be smaller for Np than U. However, as the oxidation state is decreased, the 5f- and 6d-orbitals will in principle expand. Therefore, we tentatively suggest when considering Np^{III} in relation to U^{III}, and then U^{IV}, that 5f- and 6d-orbital contraction from increasing Z_{eff} between equivalent oxidation states may be offset when moving to U with an oxidation state one unit higher (at least in the context of these An=C_{BIPM} bonding interactions). The result would be that, due to net equalization of these competing effects, Np^{III} in the An=C_{BIPM} ligand field is roughly equivalent to U^{IV} with a result that total Np contributions to the Np^{III}=C_{BIPM} bonds in **5Np** and **6Np** appears to be similar to U^{IV}=C_{BIPM} congeners, noting that the 5f orbital character dominates overall. However, the Np^{III}=C_{BIPM} σ- and π-bonds of **5Np** and **6Np** (av. 58% 5f character) exhibit a considerably less 5f character than U^{IV}=C_{BIPM} complexes (∼70−90% 5f character), which is counterbalanced for Np by increased 7s and 6d orbital participation for the σ-bonds and mainly 6d orbital participation for the π-bonds. An additional difference is the consistently significant 7s contributions (4−9%) from Np to the σ-components of the Np^{III}=C_{BIPM} bonds which has not been found for U^{IV}=C_{BIPM} bonds.

The above analysis provides a baseline from which Np^{3+}-containing **4Np−6Np** is compared to hypothetical U^{3+}-containing **4U−6U** congeners with confidence. The M−CH_{BIPM} bond orders for **4Np** and **4U** are very similar (∼0.59), with **5Np** having a higher bond order (1.40) than **5U** (1.28), but the opposite is found for **6U** (1.17) vs **6Np** (1.20). The NBO data reveal that the U ← C_{NHC} bonds are largely electrostatic and invariant, which is the same as the Np ← C_{NHC} bonds. The U^{III}=C_{BIPM} bonds are similar to the Np^{III}=C_{BIPM} bonds but slightly more polarized in terms of total metal contributions (9−14 vs 9−17%, respectively). While the π-bonds are little changed from Np^{III} to U^{III}, still having dominant 5f character (but reduced compared to U^{IV}=C_{BIPM} complexes), the σ-bonds for U have approximately equal 6d vs 5f orbital contributions but, as was found for Np, significant 7s contributions (4−10%) are revealed. Thus, it would seem that An^{III}=C_{BIPM} bonds for both An = U and Np consistently exhibit significant (∼4−10%) 7s contributions that are not present in U^{IV}=C_{BIPM} complexes. We note that the QTAIM data for **4U−6U** are quite similar to those of **4Np−6Np** and confirm the presence of U^{III}=C_{BIPM} double-bond interactions. Previously, we extrapolated bond orders and U% contributions to the U^{III}=C_{BIPM} bonds in the mixed-valent $[\{U^{III}(BIPM^{TMS})\}_3\{U^{IV}(BIPM^{TMS})\}_3(\mu\text{-}I)_3(\mu\text{-}\eta^6\text{:}\eta^6\text{-}C_7H_8)_3]$ molecule of ∼1.2 and 13%, respectively.[14] These data certainly fit well into the trends of U over oxidation states of III-VI (U^{III}, ∼13; U^{IV}, ∼18; U^{V}, ∼26; U^{VI}, ∼28%) and the data in Table 1. However, the presence of arene bridges and the large number of basis functions for $[\{U^{III}(BIPM^{TMS})\}_3\{U^{IV}(BIPM^{TMS})\}_3(\mu\text{-}I)_3(\mu\text{-}\eta^6\text{:}\eta^6\text{-}C_7H_8)_3]$ meant that these were extrapolations at best. It is thus notable that those values compare very well to the computed values for **4U−6U** (9, 14, and 14% respectively), which has been enabled with confidence by being benchmarked against **4Np−6Np**, demonstrating the value of accessing transuranium targets when U congeners are experimentally unavailable.

Next, we turn our attention to comparing the data for **4Np−6Np** to **4Ce−6Ce** because both are experimentally validated series of complexes containing central metal ions with identical Shannon ionic radii. We noted in the analysis of structural data above that the M−CH_{BIPM} bond distances are largely the same for **4Np** vs **4Ce**, but the M=C_{BIPM} and M ← C_{NHC} bonds tended to be shorter in **5Np** and **6Np** vs **5Ce** and **6Ce**. In line with those data, the computed bond metrics largely follow the same pattern, resulting in lower bond orders on a like-for-like basis for Ce (Ce−C_{BIPM} 0.46, Ce=C_{BIPM} av. 1.00, Ce ← C_{NHC} av. 0.57) vs Np (Np−C_{BIPM} 0.59, Np=C_{BIPM} av. 1.30, Np ← C_{NHC} av. 0.72). This pattern translates through to the NBO analysis, where for each system the Ce contributions (7−10%) to given polarized-covalent bonds are about 60% of the corresponding Np values (9−17%). The Ce=C_{BIPM} σ- and π-bonding components are dominated by 5d character (av. 63%), with an approximate 2:1 ratio of 5d:4f character. Also, analogously to Np, 6s character is found (1−7%) for the Ce=C_{BIPM} σ-bonds, which is significant but slightly lower than the corresponding Np 7s contributions to the Np=C_{BIPM} bonds (4−9%).

Noting the clear differences between the computed electronic structures of $5f^4$ **4Np−6Np** and $4f^1$ **4Ce−6Ce**, we finally compare isoelectronic $5f^4$ **4Np−6Np** vs $4f^4$ **4Pm−6Pm**, where the experimentally anchored calculations on **4Ce−6Ce** provide confidence in extending the models and computational methods to **4Pm−6Pm**. Notably, the computed Pm−C distances are, like-for-like, always slightly longer for **4Pm−6Pm** vs **4Np−6Np**, but, as anticipated, the Pm−C distances are shorter than the corresponding Ce−C distances because of the increased effective nuclear charge and lanthanide contraction. However, while the Np−C bond orders (0.59−1.40) are like-for-like larger than the Pm−C bond orders (0.28−0.94), the latter are also consistently lower than the corresponding Ce−C bond orders (0.46−1.05). Inspection of the NBO data of **4Pm−6Pm** reveals two notable points. First, the Pm% contributions to the Pm−CH_{BIPM} (10%) and Pm=C_{BIPM} (14−19%) bonds of **4Pm−6Pm** are similar to the Np% of the Np−CH_{BIPM} (9%) and Np=C_{BIPM} (10−17%) bonds of **4Np−6Np** and are thus significantly larger than the corresponding Ce data (7−10%). Second, whereas the Ce bonding is dominated by 5d character (av. 63%), for **4Pm−6Pm** the bonding is dominated by 4f character (av. 71%), more than the 5f character of the Np congeners (av. 56%), along with 6s contributions (1−5%). The high Pm% contributions to the bonding but low bond orders at first sight may seem contradictory, but we suggest that this is an example of 4f mixing due to a good energy match with the C_{BIPM} orbitals but poor spatial overlap.[83,84] Though the differences are small, this would appear to be the case based

https://doi.org/10.1021/jacs.2c02152
J. Am. Chem. Soc. 2022, 144, 9764−9774

on the QTAIM data, where the Pm values are consistently smaller than the Np values.

The computational results can be summarized as follows: (i) decreased f orbital contributions to bonding with M^{III} ions (relative to M^{IV} ions) can be compensated for by s and d contributions; (ii) the $Np^{III}{=}C_{BIPM}$ systems are overall comparable to $U^{IV}{=}C_{BIPM}$ analogues; (iii) Np is the most covalent (by total metal% contribution to the bonding) of Np, U, Ce, and Pm for these $M^{III}{=}C_{BIPM}$ complexes; (iv) the bonding of the Ce complexes is dominated by 5d character; (v) the bonding of the Pm complexes is dominated by 4f character, but here the covalency is likely due to good energy matching and not spatial overlap; (vi) the $M{-}C_{NHC}$ bonding is consistently highly electrostatic for all complexes; and (vii) by isolating and characterizing $Np^{III}{=}C_{BIPM}$ complexes it has been possible to complete benchmarking of U contributions in $U{=}C_{BIPM}$ bonding over U oxidation states of III-VI.

Preliminary Reactivity Assessment. A preliminary reactivity study of **5Np** reveals metallo-Wittig reactivity, as anticipated for a species with a formal Np=C double-bond interaction.[47,62,85] In particular, benzaldehyde reacts with **5Np** to afford the alkene product $PhC(H){=}C(PPh_2NSiMe_3)_2$ (**7**), Scheme 2, as evidenced by ^1H and ^{31}P NMR spectroscopic data.[62] As far as we are aware, the reaction of **5Np** with benzaldehyde constitutes the first multiple bond metathesis reaction in transuranium chemistry, and indeed An^{III}-chemistry more broadly given the dearth of An^{III}-ligand multiple bonding. The metallo-Wittig reactivity of **5Np** is complementary to the metallo-Wittig reactivity already established for U-analogues in oxidation states IV-VI,[47,62,85] showing now that An=C double bonds can execute multiple bond metathesis over the full range of commonly accessible An oxidation states (III-VI). The reactivity of **5Np** also forges a link to the metallo-Wittig reactivity of $Ln^{III}{=}C$ bonds, providing a bridge between trivalent M=C bond metathesis chemistry of Ln and An ions.

Scheme 2. Reaction of 5Np with Benzaldehyde to Produce the Alkene 7

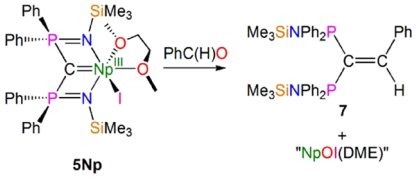

CONCLUSIONS

To conclude, we have reported the synthesis and characterization of transuranium-carbon polarized-covalent $\sigma^2\pi^2$ multiple and dative σ^2 single bond interactions. The new diphosphoniomethanide-, diphosphonio-alkylidene-, and *N*-heterocyclic carbene-neptunium(III) derivatives reported here include unambiguous examples of trivalent An-ligand multiple bonds, and their synthesis was facilitated by adopting a scaled-down prechoreographed approach using Ce^{III} synthetic surrogates. The elucidation of periodic trends across the 5f series, and comparisons to the 4f elements, is often grounded in the ability to isolate and characterize homologous series of molecules and driven by the establishment of Th and U chemistry first and subsequently followed by transuranium congeners. Consequently, the work reported here highlights an instance where nonaqueous low-valent transuranium chemistry provides the bonding motif precedent enabling comparison of M=C bonding to Ln^{III} congeners and early An=C bonding in other An oxidation states. A preliminary assessment of reactivity has introduced multiple bond metathesis to transuranium chemistry, together with prior examples of $An^{IV\text{-}VI}$ reactivity now extending the range of An metallo-Wittig reactions to encompass oxidation states III-VI overall and providing an An^{III} comparison to Ln^{III} congeners.

ASSOCIATED CONTENT

Supporting Information

The Supporting Information is available free of charge at https://pubs.acs.org/doi/10.1021/jacs.2c02152.

Experimental and computational details and X-ray crystallographic, spectroscopic, magnetic, and quantum chemical calculations (PDF)

Accession Codes

CCDC 2125323−2125331 contain the supplementary crystallographic data for this paper. These data can be obtained free of charge via www.ccdc.cam.ac.uk/data_request/cif, or by emailing data_request@ccdc.cam.ac.uk, or by contacting The Cambridge Crystallographic Data Centre, 12 Union Road, Cambridge CB2 1EZ, UK; fax: +44 1223 336033. All other data are available from the authors on reasonable request.

AUTHOR INFORMATION

Corresponding Authors

Andrew J. Gaunt − *Chemistry Division, Los Alamos National Laboratory, Los Alamos, New Mexico 87545, United States;* orcid.org/0000-0001-9679-6020; Email: gaunt@lanl.gov

Stephen T. Liddle − *Department of Chemistry and Centre for Radiochemistry Research, The University of Manchester, Manchester M13 9PL, U.K.;* orcid.org/0000-0001-9911-8778; Email: steve.liddle@manchester.ac.uk

Authors

Conrad A. P. Goodwin − *Department of Chemistry and Centre for Radiochemistry Research, The University of Manchester, Manchester M13 9PL, U.K.; Chemistry Division, Los Alamos National Laboratory, Los Alamos, New Mexico 87545, United States;* orcid.org/0000-0002-4320-2548

Ashley J. Wooles − *Department of Chemistry and Centre for Radiochemistry Research, The University of Manchester, Manchester M13 9PL, U.K.;* orcid.org/0000-0001-7411-9627

Jesse Murillo − *Chemistry Division, Los Alamos National Laboratory, Los Alamos, New Mexico 87545, United States*

Erli Lu − *Department of Chemistry and Centre for Radiochemistry Research, The University of Manchester, Manchester M13 9PL, U.K.;* orcid.org/0000-0002-0619-5967

Josef T. Boronski − *Department of Chemistry and Centre for Radiochemistry Research, The University of Manchester, Manchester M13 9PL, U.K.;* orcid.org/0000-0002-1435-6337

Brian L. Scott − *Materials Physics and Applications Division, Los Alamos National Laboratory, Los Alamos, New Mexico 87545, United States*

Complete contact information is available at: https://pubs.acs.org/10.1021/jacs.2c02152

https://doi.org/10.1021/jacs.2c02152
J. Am. Chem. Soc. 2022, 144, 9764−9774

Notes

The authors declare no competing financial interest.

■ ACKNOWLEDGMENTS

We gratefully acknowledge funding and support from the UK EPSRC (EP/P001386/1 and EP/M027015/1), EU ERC (GoG612724), U.S. Department of Energy, Office of Science, Office of Basic Energy Sciences, Chemical Sciences, Geosciences, and Biosciences Division, Heavy Element Chemistry Program at Los Alamos National Laboratory (LANL) (A.J.G., J.M., B.L.S.; contract DE-AC52-06NA25396) for experimental Np chemistry, LANL Laboratory Directed Research and Development program for a Distinguished J. R. Oppenheimer Postdoctoral Fellowship (C.A.P.G.; LANL-LDRD 20180703PRD1), and The University of Manchester including computational resources and associated support services of the Computational Shared Facility. S.T.L. thanks the Alexander von Humboldt Foundation for a Friedrich Wilhelm Bessel Research Award. We thank the anonymous referees for their constructive and helpful comments.

■ REFERENCES

(1) Hayton, T. W. Metal-ligand multiple bonding in uranium: structure and reactivity. *Dalton Trans.* **2010**, *39*, 1145−1158.
(2) Liddle, S. T. The Renaissance of Non-Aqueous Uranium Chemistry. *Angew. Chem., Int. Ed.* **2015**, *54*, 8604−8641.
(3) Hartline, D. R.; Meyer, K. From Chemical Curiosities and Trophy Molecules to Uranium-Based Catalysis: Developments for Uranium Catalysis as a New Facet in Molecular Uranium Chemistry. *JACS Au* **2021**, *1*, 698−709.
(4) Hayton, T. W. Recent developments in actinide-ligand multiple bonding. *Chem. Commun.* **2013**, *49*, 2956−2973.
(5) Brown, J. L.; Batista, E. R.; Boncella, J. M.; Gaunt, A. J.; Reilly, S. D.; Scott, B. L.; Tomson, N. C. A Linear *trans*-Bis(imido) Neptunium(V) Actinyl Analog: $Np^{V}(NDipp)_2(^{t}Bu_2bipy)_2Cl$ (Dipp = 2,6-$^{i}Pr_2C_6H_3$). *J. Am. Chem. Soc.* **2015**, *137*, 9583−9586.
(6) Dutkiewicz, M. S.; Goodwin, C. A. P.; Perfetti, M.; Gaunt, A. J.; Griveau, J.-C.; Colineau, E.; Kovács, A.; Wooles, A. J.; Caciuffo, R.; Walter, O.; Liddle, S. T. A Terminal Neptunium(V)-Mono(Oxo) Complex. *Nat. Chem.* **2022**, *14*, 342−349.
(7) Pereira, C. C.; Marsden, C. J.; Marçalo, J.; Gibson, J. K. Actinide sulfides in the gas phase: experimental and theoretical studies of the thermochemistry of AnS (An = Ac, Th, Pa, U, Np, Pu, Am and Cm). *Phys. Chem. Chem. Phys.* **2011**, *13*, 12940−12958.
(8) Infante, I.; Kovacs, A.; La Macchia, G.; Shahi, A. R.; Gibson, J. K.; Gagliardi, L. Ionization energies for the actinide mono- and dioxides series, from Th to Cm: theory versus experiment. *J. Phys. Chem. A* **2010**, *114*, 6007−6015.
(9) Marçalo, J.; Gibson, J. K. Gas-phase energetics of actinide oxides: an assessment of neutral and cationic monoxides and dioxides from thorium to curium. *J. Phys. Chem. A* **2009**, *113*, 12599−12606.
(10) Gibson, J. K.; Haire, R. G.; Marçalo, J.; Santos, M.; Pires de Matos, A.; Mrozik, M. K.; Pitzer, R. M.; Bursten, B. E. Gas-Phase Reactions of Hydrocarbons with An^+ and AnO^+ (An = Th, Pa, U, Np, Pu, Am, Cm): The Active Role of 5f Electrons in Organoprotactinium Chemistry. *Organometallics* **2007**, *26*, 3947−3956.
(11) Gibson, J. K. Actinide Gas-Phase Chemistry: Reactions of An^+ and AnO^+ [An = Th, U, Np, Pu, Am] with Nitriles and Butylamine. *Inorg. Chem.* **1999**, *38*, 165−173.
(12) Gibson, J. K. Gas-Phase Transuranium Organometallic Chemistry: Reactions of Np^+, Pu^+, NpO^+, and PuO^+ with Alkenes. *J. Am. Chem. Soc.* **1998**, *120*, 2633−2640.
(13) Kovács, A.; Konings, R. J. M.; Gibson, J. K.; Infante, I.; Gagliardi, L. Quantum chemical calculations and experimental investigations of molecular actinide oxides. *Chem. Rev.* **2015**, *115*, 1725−1759.
(14) Wooles, A. J.; Mills, D. P.; Tuna, F.; McInnes, E. J. L.; Law, G. T. W.; Fuller, A. J.; Kremer, F.; Ridgway, M.; Lewis, W.; Gagliardi, L.; Vlaisavljevich, B.; Liddle, S. T. Uranium(III)-carbon multiple bonding supported by arene δ-bonding in mixed-valence hexauranium nanometre-scale rings. *Nat. Commun.* **2018**, *9*, 2097.
(15) Long, B. N.; Beltrán-Leiva, M. J.; Celis-Barros, C.; Sperling, J. M.; Poe, T. N.; Baumbach, R. E.; Windorff, C. J.; Albrecht-Schönzart, T. E. Cyclopentadienyl coordination induces unexpected ionic Am-N bonding in an americium bipyridyl complex. *Nat. Commun.* **2022**, *13*, 201.
(16) Zwick, B. D.; Sattelberger, A. P.; Avens, L. R. Transuranium Organometallics Elements: The Next Generation. In *Transuranium Elements: A Half Century*, Morss, L. R.; Fuger, J., Eds.; American Chemical Society: Washington DC, 1992; 239−247.
(17) Marks, T. J.; Fischer, R. D., Eds. *Organometallics of the f-Elements: Proceedings of the NATO Advanced Study Institute, Sogesta, Urbino, Italy, Sept, 1978*; Springer: Dordrecht, 1978.
(18) De Ridder, D. J. A.; Rebizant, J.; Apostolidis, C.; Kanellakopulos, B.; Dornberger, E. Bis(cyclooctatetraenyl)-neptunium(IV). *Acta Crystallogr. C* **1996**, *52*, 597−600.
(19) Magnani, N.; Apostolidis, C.; Morgenstern, A.; Colineau, E.; Griveau, J. C.; Bolvin, H.; Walter, O.; Caciuffo, R. Magnetic memory effect in a transuranic mononuclear complex. *Angew. Chem., Int. Ed.* **2011**, *50*, 1696−1698.
(20) Walter, O. Actinide Organometallic Complexes with π-Ligands. *Chem. − Eur. J.* **2019**, *25*, 2927−2934.
(21) Arnold, P. L.; Dutkiewicz, M. S.; Walter, O. Organometallic Neptunium Chemistry. *Chem. Rev.* **2017**, *117*, 11460−11475.
(22) Goodwin, C. A. P.; Su, J.; Stevens, L. M.; White, F. D.; Anderson, N. H.; Auxier, J. D., II; Albrecht-Schönzart, T. E.; Batista, E. R.; Briscoe, S. F.; Cross, J. N.; Evans, W. J.; Gaiser, A. N.; Gaunt, A. J.; James, M. R.; Janicke, M. T.; Jenkins, T. F.; Jones, Z. R.; Kozimor, S. A.; Scott, B. L.; Sperling, J. M.; Wedal, J. C.; Windorff, C. J.; Yang, P.; Ziller, J. W. Isolation and Characterization of a Californium Metallocene. *Nature* **2021**, *599*, 421−424.
(23) Karraker, D. G.; Stone, J. A. Bis(cyclooctatetraenyl)neptunium-(III) and -plutonium(III) compounds. *J. Am. Chem. Soc.* **1974**, *96*, 6885−6888.
(24) Karraker, D. G.; Stone, J. A.; Jones, E. R.; Edelstein, N. Bis(cyclooctatetraenyl)neptunium(IV) and bis(cyclooctatetraenyl)-plutonium(IV). *J. Am. Chem. Soc.* **1970**, *92*, 4841−4845.
(25) Windorff, C. J.; Sperling, J. M.; Albrecht-Schönzart, T. E.; Bai, Z.; Evans, W. J.; Gaiser, A. N.; Gaunt, A. J.; Goodwin, C. A. P.; Hobart, D. E.; Huffman, Z. K.; Huh, D. N.; Klamm, B. E.; Poe, T. N.; Warzecha, E. A Single Small-Scale Plutonium Redox Reaction System Yields Three Crystallographically-Characterizable Organoplutonium Complexes. *Inorg. Chem.* **2020**, *59*, 13301−13314.
(26) Apostolidis, C.; Walter, O.; Vogt, J.; Liebing, P.; Maron, L.; Edelmann, F. T. A Structurally Characterized Organometallic Plutonium(IV) Complex. *Angew. Chem., Int. Ed.* **2017**, *56*, 5066−5070.
(27) Su, J.; Windorff, C. J.; Batista, E. R.; Evans, W. J.; Gaunt, A. J.; Janicke, M. T.; Kozimor, S. A.; Scott, B. L.; Woen, D. H.; Yang, P. Identification of the Formal +2 Oxidation State of Neptunium: Synthesis and Structural Characterization of $\{Np^{II}[C_5H_3(SiMe_3)_2]_3\}^{1-}$. *J. Am. Chem. Soc.* **2018**, *140*, 7425−7428.
(28) Windorff, C. J.; Chen, G. P.; Cross, J. N.; Evans, W. J.; Furche, F.; Gaunt, A. J.; Janicke, M. T.; Kozimor, S. A.; Scott, B. L. Identification of the Formal +2 Oxidation State of Plutonium: Synthesis and Characterization of $\{Pu^{II}[C_5H_3(SiMe_3)_2]_3\}^{-}$. *J. Am. Chem. Soc.* **2017**, *139*, 3970−3973.
(29) Apostolidis, C.; Dutkiewicz, M. S.; Kovács, A.; Walter, O. Solid-State Structure of Tris-Cyclopentadienide Uranium(III) and Plutonium(III). *Chem. − Eur. J.* **2018**, *24*, 2841−2844.
(30) Dutkiewicz, M. S.; Farnaby, J. H.; Apostolidis, C.; Colineau, E.; Walter, O.; Magnani, N.; Gardiner, M. G.; Love, J. B.; Kaltsoyannis, N.; Caciuffo, R.; Arnold, P. L. Organometallic neptunium(III) complexes. *Nat. Chem.* **2016**, *8*, 797−802.

https://doi.org/10.1021/jacs.2c02152
J. Am. Chem. Soc. 2022, 144, 9764−9774

(31) Laubereau, P. G. The formation of dicyclopentadienylberkeliumchloride. *Inorg. Nucl. Chem. Lett.* **1970**, *6*, 611−616.
(32) Bagnall, K. W.; Payne, G. F.; Alcock, N. W.; Flanders, D. J.; Brown, D. Actinide structural studies. Part 8. Some new oxygen-donor complexes of trichloro(cyclopentadienyl)neptunium(IV); the crystal structure of trichloro(η^5-cyclopentadienyl)bis-(methyldiphenylphosphine oxide)neptunium(IV). *J. Chem. Soc., Dalton Trans.* **1986**, 783−787.
(33) Bagnall, K. W.; Plews, M. J.; Brown, D.; Fischer, R. D.; Klähne, E.; Landgraf, G. W.; Sienel, G. R. Anionic tris(cyclopentadienyl)-actinide(IV) complexes. *J. Chem. Soc., Dalton Trans.* **1982**, 1999−2007.
(34) Bagnall, K. W.; Plews, M. J.; Brown, D. Tris(cyclopentadienyl)-plutonium(IV) chloride and thiocyanate, (η^5-C_5H_5)$_3$PuCl and (η^5-C_5H_5)$_3$Pu(NCS). *J. Organomet. Chem.* **1982**, *224*, 263−266.
(35) Bagnall, K. W.; Payne, G. F.; Brown, D. Phosphine oxide complexes of cyclopentadienyl neptunium(IV) and plutonium(IV) *N*-thiocyanates. *J. Less Common Met.* **1986**, *116*, 333−339.
(36) Karraker, D. G.; Stone, J. A. Covalency of neptunium(IV) tris(cyclopentadienyl) compounds from Mössbauer spectra. *Inorg. Chem.* **1979**, *18*, 2205−2207.
(37) Karraker, D. G. Reaction of Plutonium Metal with Diiodoethane. In *Plutonium Chemistry*; American Chemical Society: 1983; *216*, 41−48.
(38) Staun, S. L.; Stevens, L. M.; Smiles, D. E.; Goodwin, C. A. P.; Billow, B. S.; Scott, B. L.; Wu, G.; Tondreau, A. M.; Gaunt, A. J.; Hayton, T. W. Expanding the Nonaqueous Chemistry of Neptunium: Synthesis and Structural Characterization of [Np(NR$_2$)$_3$Cl], [Np(NR$_2$)$_3$Cl]$^-$, and [Np{N(R)(SiMe$_2$CH$_2$)}$_2$(NR$_2$)]$^-$ (R = SiMe$_3$). *Inorg. Chem.* **2021**, *60*, 2740−2748.
(39) Myers, A. J.; Tarlton, M. L.; Kelley, S. P.; Lukens, W. W.; Walensky, J. R. Synthesis and Utility of Neptunium(III) Hydrocarbyl Complex. *Angew. Chem., Int. Ed.* **2019**, *58*, 14891−14895.
(40) de Frémont, P.; Marion, N.; Nolan, S. P. Carbenes: Synthesis, properties, and organometallic chemistry. *Coord. Chem. Rev.* **2009**, *253*, 862−892.
(41) Ephritikhine, M. Uranium carbene compounds. *C. R. Chim.* **2013**, *16*, 391−405.
(42) Nelson, D. J.; Nolan, S. P. Quantifying and understanding the electronic properties of N-heterocyclic carbenes. *Chem. Soc. Rev.* **2013**, *42*, 6723−6753.
(43) Herrmann, W. A.; Köcher, C. N-Heterocyclic Carbenes. *Angew. Chem., Int. Ed.* **1997**, *36*, 2162−2187.
(44) Bourissou, D.; Guerret, O.; Gabbaï, F. P.; Bertrand, G. Stable Carbenes. *Chem. Rev.* **2000**, *100*, 39−92.
(45) Hopkinson, M. N.; Richter, C.; Schedler, M.; Glorius, F. An overview of N-heterocyclic carbenes. *Nature* **2014**, *510*, 485−496.
(46) Cramer, R. E.; Maynard, R. B.; Paw, J. C.; Gilje, J. W. A uranium-carbon multiple bond. Crystal and molecular structure of (η^5-C_5H_5)$_3$UCHP(CH$_3$)$_2$(C_6H_5). *J. Am. Chem. Soc.* **1981**, *103*, 3589−3590.
(47) Gregson, M.; Wooles, A. J.; Cooper, O. J.; Liddle, S. T. Covalent Uranium Carbene Chemistry. *Comments Inorg. Chem.* **2015**, *35*, 262−294.
(48) Liddle, S. T.; Mills, D. P.; Wooles, A. J. Early metal bis(phosphorus-stabilised)carbene chemistry. *Chem. Soc. Rev.* **2011**, *40*, 2164−2176.
(49) Lu, E.; Wooles, A. J.; Gregson, M.; Cobb, P. J.; Liddle, S. T. A Very Short Uranium(IV)-Rhodium(I) Bond with Net Double-Dative Bonding Character. *Angew. Chem., Int. Ed.* **2018**, *57*, 6587−6591.
(50) Lu, E.; Boronski, J. T.; Gregson, M.; Wooles, A. J.; Liddle, S. T. Silyl-Phosphino-Carbene Complexes of Uranium(IV). *Angew. Chem., Int. Ed.* **2018**, *57*, 5506−5511.
(51) Lu, E.; Atkinson, B. E.; Wooles, A. J.; Boronski, J. T.; Doyle, L. R.; Tuna, F.; Cryer, J. D.; Cobb, P. J.; Vitorica-Yrezabal, I. J.; Whitehead, G. F. S.; Kaltsoyannis, N.; Liddle, S. T. Back-bonding between an electron-poor, high-oxidation-state metal and poor π-acceptor ligand in a uranium(V)-dinitrogen complex. *Nat. Chem.* **2019**, *11*, 806−811.
(52) Seed, J. A.; Sharpe, H. R.; Futcher, H. J.; Wooles, A. J.; Liddle, S. T. Nature of the Arsonium-Ylide Ph$_3$As=CH$_2$ and a Uranium(IV) Arsonium-Carbene Complex. *Angew. Chem., Int. Ed.* **2020**, *59*, 15870−15874.
(53) Kent, G. T.; Yu, X.; Wu, G.; Autschbach, J.; Hayton, T. W. Synthesis and electronic structure analysis of the actinide allenylidenes, [{(NR$_2$)$_3$}An(CCCPh$_2$)]$^-$ (An = U, Th; R = SiMe$_3$). *Chem. Sci.* **2021**, *12*, 14383−14388.
(54) Arnold, P. L.; Casely, I. J. F-block N-heterocyclic carbene complexes. *Chem. Rev.* **2009**, *109*, 3599−3611.
(55) Oldham Jr, W. J.; Oldham, S. M.; Smith, W. H.; Costa, D. A.; Scott, B. L.; Abney, K. D., Synthesis and structure of *N*-heterocyclic carbene complexes of uranyl dichloride. *Chem. Commun.* **2001**, 1348−1349.
(56) Nakai, H.; Hu, X.; Zakharov, L. N.; Rheingold, A. L.; Meyer, K. Synthesis and characterization of *N*-heterocyclic carbene complexes of uranium(III). *Inorg. Chem.* **2004**, *43*, 855−857.
(57) Evans, W. J.; Kozimor, S. A.; Ziller, J. W. Bis(pentamethylcyclopentadienyl) U(III) oxide and U(IV) oxide carbene complexes. *Polyhedron* **2004**, *23*, 2689−2694.
(58) Gardner, B. M.; McMaster, J.; Liddle, S. T. Synthesis and structure of a bis-N-heterocyclic carbene complex of uranium tetrachloride exhibiting short Cl···C$_{carbene}$ contacts. *Dalton Trans.* **2009**, 6924−6926.
(59) Seed, J. A.; Gregson, M.; Tuna, F.; Chilton, N. F.; Wooles, A. J.; McInnes, E. J. L.; Liddle, S. T. Rare-Earth- and Uranium-Mesoionic Carbenes: A New Class of f-Block Carbene Complex Derived from an N-Heterocyclic Olefin. *Angew. Chem., Int. Ed.* **2017**, *56*, 11534−11538.
(60) Cooper, O. J.; Mills, D. P.; McMaster, J.; Moro, F.; Davies, E. S.; Lewis, W.; Blake, A. J.; Liddle, S. T. Uranium-carbon multiple bonding: facile access to the pentavalent uranium carbene [U{C(PPh$_2$NSiMe$_3$)$_2$}(Cl)$_2$(I)] and comparison of U^V=C and U^{IV}=C bonds. *Angew. Chem., Int. Ed.* **2011**, *50*, 2383−2386.
(61) Mills, D. P.; Moro, F.; McMaster, J.; van Slageren, J.; Lewis, W.; Blake, A. J.; Liddle, S. T. A delocalized arene-bridged diuranium single-molecule magnet. *Nat. Chem.* **2011**, *3*, 454−460.
(62) Mills, D. P.; Cooper, O. J.; Tuna, F.; McInnes, E. J.; Davies, E. S.; McMaster, J.; Moro, F.; Lewis, W.; Blake, A. J.; Liddle, S. T. Synthesis of a uranium(VI)-carbene: reductive formation of uranyl(V)-methanides, oxidative preparation of a [R$_2$C=U=O]$^{2+}$ analogue of the [O=U=O]$^{2+}$ uranyl ion (R = Ph$_2$PNSiMe$_3$), and comparison of the nature of U^{IV}=C, U^V=C, and U^{VI}=C double bonds. *J. Am. Chem. Soc.* **2012**, *134*, 10047−10054.
(63) Morss, L. R.; Edelstein, N. M.; Fuger, J. (Eds), *The Chemistry of the Actinide and Transactinide Elements*; Springer: Dordrecht, 2011.
(64) Goodwin, C. A. P.; Janicke, M. T.; Scott, B. L.; Gaunt, A. J. [AnI$_3$(THF)$_4$] (An = Np, Pu) preparation bypassing An^0 metal precursors: access to Np^{3+}/Pu^{3+} nonaqueous and organometallic complexes. *J. Am. Chem. Soc.* **2021**, *143*, 20680−20696.
(65) Gregson, M.; Lu, E.; McMaster, J.; Lewis, W.; Blake, A. J.; Liddle, S. T. A cerium(IV)-carbon multiple bond. *Angew. Chem., Int. Ed.* **2013**, *52*, 13016−13019.
(66) Talavera, G.; Peña, J.; Alcarazo, M. Dihalo(imidazolium)-sulfuranes: A Versatile Platform for the Synthesis of New Electrophilic Group-Transfer Reagents. *J. Am. Chem. Soc.* **2015**, *137*, 8704−8707.
(67) Ansell, M. B.; Roberts, D. E.; Cloke, F. G.; Navarro, O.; Spencer, J. Synthesis of an [(NHC)$_2$Pd(SiMe$_3$)$_2$] Complex and Catalytic *cis*-Bis(silyl)ations of Alkynes with Unactivated Disilanes. *Angew. Chem., Int. Ed.* **2015**, *54*, 5578−5582.
(68) Kihara, S.; Yoshida, Z.; Aoyagi, H.; Maeda, K.; Shirai, O.; Kitatsuji, Y.; Yoshida, Y. A Critical Evaluation of the Redox Properties of Uranium, Neptunium and Plutonium Ions in Acidic Aqueous Solutions. *Pure Appl. Chem.* **1999**, *71*, 1771−1807.
(69) Jones, M. B.; Gaunt, A. J.; Gordon, J. C.; Kaltsoyannis, N.; Neu, M. P.; Scott, B. L. Uncovering f-element bonding differences and electronic structure in a series of 1 : 3 and 1 : 4 complexes with a diselenophosphinate ligand. *Chem. Sci.* **2013**, *4*, 1189−1203.

https://doi.org/10.1021/jacs.2c02152
J. Am. Chem. Soc. 2022, 144, 9764−9774

(70) Macor, J. A.; Brown, J. L.; Cross, J. N.; Daly, S. R.; Gaunt, A. J.; Girolami, G. S.; Janicke, M. T.; Kozimor, S. A.; Neu, M. P.; Olson, A. C.; Reilly, S. D.; Scott, B. L. Coordination chemistry of 2,2′-biphenylenedithiophosphinate and diphenyldithiophosphinate with U, Np, and Pu. *Dalton Trans.* **2015**, *44*, 18923−18936.
(71) Su, J.; Cheisson, T.; McSkimming, A.; Goodwin, C. A. P.; DiMucci, I. M.; Albrecht-Schönzart, T.; Scott, B. L.; Batista, E. R.; Gaunt, A. J.; Kozimor, S. A.; Yang, P.; Schelter, E. J. Complexation and redox chemistry of neptunium, plutonium and americium with a hydroxylaminato ligand. *Chem. Sci.* **2021**, *12*, 13343−13359.
(72) Wilson, R. E.; Carter, T. J.; Autillo, M.; Stegman, S. Thiocyanate complexes of the lanthanides, Am and Cm. *Chem. Commun.* **2020**, *56*, 2622−2625.
(73) Shannon, R. D. Revised effective ionic radii and systematic studies of interatomic distances in halides and chalcogenides. *Acta Crystallogr. A* **1976**, *32*, 751−767.
(74) Orzechowski, L.; Jansen, G.; Harder, S. Synthesis, Structure, and Reactivity of a Stabilized Calcium Carbene: R_2CCa. *J. Am. Chem. Soc.* **2006**, *128*, 14676−14684.
(75) Lu, E.; Cooper, O. J.; Tuna, F.; Wooles, A. J.; Kaltsoyannis, N.; Liddle, S. T. Uranium-Carbene-Imido Metalla-Allenes: Ancillary-Ligand-Controlled *cis*-/*trans*-Isomerisation and Assessment of *trans* Influence in the $R_2C{=}U^{IV}{=}NR'$ Unit ($R{=}Ph_2PNSiMe_3$; $R'{=}CPh_3$). *Chem. − Eur. J.* **2016**, *22*, 11559−11563.
(76) Lu, E.; Tuna, F.; Lewis, W.; Kaltsoyannis, N.; Liddle, S. T. Uranium Metalla-Allenes with Carbene Imido $R_2C{=}U^{IV}{=}NR'$ Units ($R{=}Ph_2PNSiMe_3$; $R'{=}CPh_3$): Alkali-Metal-Mediated Push-Pull Effects with an Amido Auxiliary. *Chem. − Eur. J.* **2016**, *22*, 11554−11558.
(77) Gregson, M.; Lu, E.; Mills, D. P.; Tuna, F.; McInnes, E. J.; Hennig, C.; Scheinost, A. C.; McMaster, J.; Lewis, W.; Blake, A. J.; Kerridge, A.; Liddle, S. T. The inverse-*trans*-influence in tetravalent lanthanide and actinide *bis*(carbene) complexes. *Nat. Commun.* **2017**, *8*, 14137.
(78) Goodwin, C. A. P.; Ciccone, S. R.; Bekoe, S.; Majumdar, S.; Scott, B. L.; Ziller, J. W.; Gaunt, A. J.; Furche, F.; Evans, W. J. 2.2.2-Cryptand complexes of neptunium(III) and plutonium(III). *Chem. Commun.* **2022**, *58*, 997−1000.
(79) Carnall, W. T. A systematic analysis of the spectra of trivalent actinide chlorides in D_{3h} site symmetry. *J. Chem. Phys.* **1992**, *96*, 8713−8726.
(80) Apostolidis, C.; Schimmelpfennig, B.; Magnani, N.; Lindqvist-Reis, P.; Walter, O.; Sykora, R.; Morgenstern, A.; Colineau, E.; Caciuffo, R.; Klenze, R.; Haire, R. G.; Rebizant, J.; Bruchertseifer, F.; Fanghänel, T. $[An(H_2O)_9](CF_3SO_3)_3$ (An=U-Cm, Cf): Exploring Their Stability, Structural Chemistry, and Magnetic Behavior by Experiment and Theory. *Angew. Chem., Int. Ed.* **2010**, *49*, 6343−6347.
(81) Carnall, W. T.; Crosswhite, H.; Crosswhite, H. M.; Hessler, J. P.; Edelstein, N.; Conway, J. G.; Shalimoff, G. V.; Sarup, R. Energy level analysis of Np^{3+}:$LaCl_3$ and Np^{3+}:$LaBr_3$. *J. Chem. Phys.* **1980**, *72*, 5089−5102.
(82) Bader, R. F. W.; Slee, T. S.; Cremer, D.; Kraka, E. Description of conjugation and hyperconjugation in terms of electron distributions. *J. Am. Chem. Soc.* **1983**, *105*, 5061−5068.
(83) Kirker, I.; Kaltsoyannis, N. Does covalency *really* increase across the 5f series? A comparison of molecular orbital, natural population, spin and electron density analyses of $AnCp_3$ (An = Th-Cm; Cp = η^5-C_5H_5). *Dalton Trans.* **2011**, *40*, 124−131.
(84) Su, J.; Batista, E. R.; Boland, K. S.; Bone, S. E.; Bradley, J. A.; Cary, S. K.; Clark, D. L.; Conradson, S. D.; Ditter, A. S.; Kaltsoyannis, N.; Keith, J. M.; Kerridge, A.; Kozimor, S. A.; Löble, M. W.; Martin, R. L.; Minasian, S. G.; Mocko, V.; La Pierre, H. S.; Seidler, G. T.; Shuh, D. K.; Wilkerson, M. P.; Wolfsberg, L. E.; Yang, P. Energy-Degeneracy-Driven Covalency in Actinide Bonding. *J. Am. Chem. Soc.* **2018**, *140*, 17977−17984.
(85) Cooper, O. J.; Mills, D. P.; Lewis, W.; Blake, A. J.; Liddle, S. T. Reactivity of the uranium(IV) carbene complex $[U(BIPM^{TMS})(Cl)(\mu\text{-}Cl)_2Li(THF)_2]$ ($BIPM^{TMS}$ = $\{C(PPh_2NSiMe_3)_2\}$) towards carbonyl and heteroallene substrates: metallo-Wittig, adduct formation, C-F bond activation, and [2 + 2]-cycloaddition reactions. *Dalton Trans.* **2014**, *43*, 14275−14283.

https://doi.org/10.1021/jacs.2c02152
J. Am. Chem. Soc. 2022, 144, 9764−9774